Evaluation of divergence-free correction algorithms in high resolution 4-D flow images of cranial vasculature.

Michael Loecher[1], Steven Kecskemeti[2], Kevin M Johnson[1], Patrick Turski[3], and Oliver Wieben[1,3]

[1]*Medical Physics, University of Wisconsin Madison, Madison, WI, United States,* [2]*Physics, University of Wisconsin Madison, Madison, WI, United States,* [3]*Radiology, University of Wisconsin Madison, Madison, WI, United States*

Introduction 4D MR flow imaging is often limited by low velocity-to-noise (VNR) ratios due to the temporal and spatial resolutions required to cover a large imaging volume with a broad range of velocities of interest in a reasonable amount of time. With blood flow imaging, we can utilize physical characteristics of blood to constrain our velocity fields to realistic values. One of these constraints is to remove divergence from the velocity images, based on the knowledge that blood is incompressible and therefore should not display any divergence. One can then assume that any divergence in the blood flow field is coming from noise, and its removal will reduce noise in the data. This study measures noise reduction in 4D MR flow images acquired in a flow phantom and in vivo in the internal carotid arteries when coupled with two methods that have been shown to work in phase contrast imaging: a finite difference (FDM) based method and a radial basis function (RBF) based method. The comparison includes an analysis of noise and visualization features when using these correction algorithms with 4D MR flow images in vascular territories with medium to small vessels and low VNR.

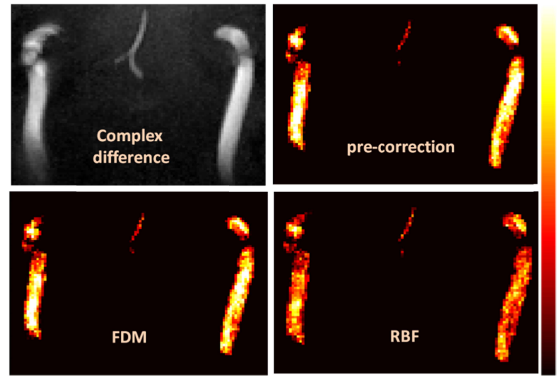

Figure 1: Noise maps in a coronal slice through the internal carotids calculated as the standard deviation of the surrounding 3x3x3 cube of voxels, from a difference image between two subsequent scans. The noise levels are seen to decrease, particularly with the RBF method.

Algorithms The FDM algorithm [1] solves for a divergence free field Pv, where $Pv = v - \nabla p$, given $\nabla^2 \mathrm{p} = \nabla \cdot \mathrm{v}$. It is solved by taking the gradient of the velocity field, applying an inverse 7-point Laplacian, calculating the divergence of the result, and then subtracting this from the acquired velocity field. The inverse Laplacian is solved with a fast sine transform. The RBF method [2-3] takes a radial basis function, which in our case is a Gaussian function ($\psi(\boldsymbol{r}) = e^{-\varepsilon \boldsymbol{r}^2}$), and creates an interpolation matrix made up of divergent free radial basis functions. This interpolation matrix is defined as $\boldsymbol{\Phi}(\boldsymbol{r}) = \{\nabla\nabla^{\mathrm{T}} - \nabla^2 \boldsymbol{I}\}\psi(\boldsymbol{r})$ where $\boldsymbol{\Phi}(\boldsymbol{r})$ is the interpolation matrix and $\psi(\boldsymbol{r})$ is the initial radial basis function. This matrix is fit to the data with LSQR fitting in Matlab (Mathworks, Natick, MA). A normalized convolution is included to prevent fitting to data outside of the vessel.

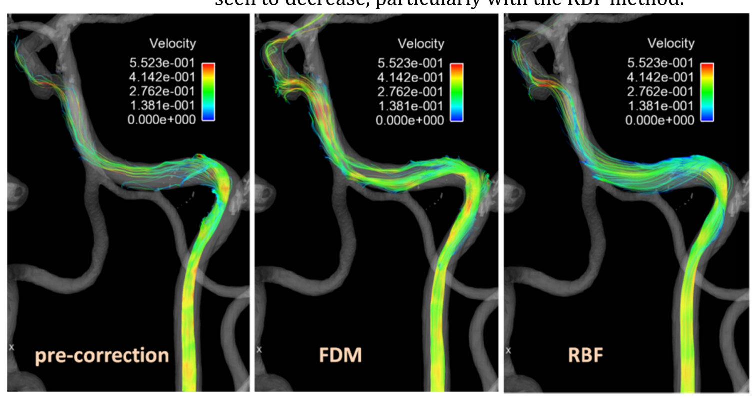

Figure 2: Streamlines through the right internal carotid of a volunteer before and after each of the corrections. The streamlines are longer and more consistent after the divergence free algorithms are applied.

Methods MR flow data were acquired in a straight tube flow phantom and the internal carotid arteries of a volunteer on a clinical 3T scanner (Discovery 750, GE Healthcare, Waukesha, WI) with a 3D radially undersampled acquisition (PC-VIPR) [4] with the following parameters: acquired isotropic spatial resolution = 0.68 mm, TR/TE = 8.3/2.9 ms, VENC = 800 mm/s, 36-38 cardiac phases, temporal resolution = 30 ms with radial view sharing [5]. Reference datasets with high SNR were reconstructed with 40,000 (phantom) and 32,000 (in vivo) projection angles. In subsequent scans, data were acquired in 25% of the previous scan with 10,000 projections for the phantom scan and 8,000 projections for the in vivo scan. A second pair of in vivo images was taken with 8,000 projections each to measure noise from the difference image. These data were reconstructed without imposing divergence free conditions and with the FDM and the RBF method. For in vivo comparisons, the image volumes were mutually registered with FLIRT (FMRIB, Oxford, UK) to compensate for any motion between the scans. For the high-low SNR pairs, the RMSE between the images from the long and the short acquisition were compared by an RMSE analysis. A noise reduction factor F was calculated as [equation 1], where 1 represents no noise reduction and 0 would represent identity with the longer reference scan. Noise levels were also measured as the standard deviation (σ_v) from the difference image explained above, across a large vessel ROI and in a convolved 3x3x3 segment to create maps. Streamlines were generated with Ensight (CEI, Apex, NC) from 500 emitters in a proximal slice in the carotid artery. Visualization improvement was compared by calculating the average streamline length with a customized Matlab routine.

$$F = \frac{\left\| v_{4x} - divfree(v_{1x}) \right\|_2}{\left\| v_{4x} - v_{1x} \right\|_2} \quad (1)$$

Results In the flow phantom, the RMSE analysis resulted in F = .94 for the FDM method, and F = .85 with the RBF method. In the carotid artery images, the error analysis resulted in F = .93 with the FDM algorithm, and F= .79 with the RBF method. The standard deviation measurements in the internal carotid images showed a reduction of .95 for the FDM method, and .74 for the RBF method. Maps of standard deviation for the in vivo scan are shown in Fig. 1. Average streamline lengths were 4.4cm in the original dataset, 5.7cm after FDM correction, and 5.4cm after RBF correction (see Fig 2).

Discussion Our study shows that imposing divergence free conditions to 4D MR flow data is a viable option for noise reductions as both the FDM and RBF methods show a decrease in noise in the velocity fields. The RMSE measurements show significant improvements with the application of divergence free algorithms, particularly with the RBF based method. This RMSE measurement does not represent true error because the images from extended scan times still contain noise and some aliasing from radial undersampling, yet they do represent datasets with significantly reduced noise contributions. Direct velocity-field noise measurements show very similar improvements compared to the RMSE calculations. Overall the RBF method shows a significantly higher noise reduction. Both algorithms also increased streamline lengths in the phantom data, with the FDM method performing slightly better. The reasons for the strong FDM performance in comparison to its noise performance are unclear, and will be investigated further. It is important to note that both of these algorithms provide higher gains in low SNR data, as similar measurements in images with higher SNR provided less significant gains. Future work will involve investigating other implementations of the RBF method, where different basis functions are used, and noise is considered in the interpolation. It will also be interesting to compare the methods in larger arteries such as the aorta, where they might work better because derivatives are easier to calculate.

References **[1]** SM Song, *et al.* JMRI 1993; 3(4) 587-96 **[2]** S Lowitsch, *Texas A&M University* 2002 **[3]** J Busch *et al.* ISMRM 2011; 1201 **[4]** KM Johnson, *et al*. MRM 2008; 60:1329-1336 **[5]** J Liu, *et al*. IEEE Tr Med Im 2006; 25(2):148-157.

Acknowledgements We gratefully acknowledge funding by NIH grant 2R01HL072260 and GE Healthcare for their assistance and support.